Volt-VAR-Pressure Optimization of Integrated Energy Systems with Hydrogen Injection

Pengfei Zhao, Xi Lu, Chenghong Gu, *Member, IEEE*, Qian Ai, *Senior Member, IEEE*, Hong Liu, *Member, IEEE*, Zhidong Cao, Yuankai Bian and Shuangqi Li

***Abstract*—Volt-VAR optimization (VVO) has been investigated extensively in power systems. However, under the era of integrated energy systems (IES), the growing interdependencies between different energy systems complicate traditional VVO. This is further hardened by incurred gas quality problems due to the hydrogen injection in IES, produced by widely applied power-to-gas (P2G) facilitates that couple between power and gas systems. This paper develops a two-stage volt-VAR-pressure optimization (VVPO) model for PV-penetrated IES to manage the variation of system voltages while managing gas quality indices. In addition to the traditional voltage regulating devices, P2G facilities, which can mitigate fluctuating PV output via converting the surplus generation into hydrogen, are also used for voltage management. A two-stage distributionally robust optimization (DRO) based on moment information is utilized to model PV uncertainty. A semidefinite programming model is formulated and finally solved by the constraint generation algorithm. A 33-bus-20-node IES is used to verify the effectiveness of the proposed VVPO on voltage management, ensured gas quality with high economic efficiency. The proposed VVPO is applicable to injecting other green gases into gas systems while ensuring power quality and enable system operators to provide low-cost but high-quality multi-energy to customers.**

***Index Terms*—Integrated energy systems, gas quality, renewable uncertainty, two-stage distributionally robust optimization, volt-VAR optimization.**

NOMENCLATURE

A. Indices and sets

t, T	Index and set for time periods.
b , B	Index and set for power buses.
n, N	Index and set for nodes in gas system.
i_e, I_e	Index and set for traditional distributed generators (DG).
i_g, I_g	Index and set for natural gas sources.
gt,GT	Index and set for gas turbines.
j, J	Index and set for PV systems.
l_e, L_e	Index and set for power lines.
l_g, L_g	Index and set for gas pipelines.
k_e, K_e	Index and set for electric loads.
k_g, K_g	Index and set for gas loads.

B. Abbreviations

CP	Combustion potential.
DG	Distributed generator.
DRO	Distributionally robust optimization.
DR-VVPO	Distributionally robust- Volt-VAR-pressure optimization.
GCV	Gross calorific value.
G2P	Gas-to-power.
LPG	Liquid petroleum gas.
OLTC	On-load tap changer.
P2G	Power-to-gas.
RO	Robust optimization.
SG	Specific gravity.
SO	Stochastic Optimization.
VVO	Volt-VAR optimization.
VVPO	Volt-VAR-pressure optimization.
WI	Wobbe index.

C. Parameters

$P_{sub,max}$	Maximum active power transfer of substation.
$R_{i_e}^{+}$, $R_{i_e}^{-}$	Maximum up and down reserve capacity of traditional DG i_e at time *t*.
R_{gt}^{+}, R_{gt}^{-}	Maximum up and down reserve capacity of gas turbine *gt* at time t.
$P_{i_e,max}$, $P_{i_e,min}$	Maximum and minimum output of tradiational DG i_e.
$P_{i_g,max}P_{i_g,min}$	Maximum and minimum output of natural gas source i_g.
$P_{gt,max}P_{gt,min}$	Maximum and minimum output of gas turbine *gt*.
$V_{b,max}, V_{b,min}$	Maximum and minimum voltage limit.
δ^{OLTC}	Size of change for each step in OLTC tap position.
nTP_{max}^{OLTC}	Maximum allowed number of switching operations of OLTC.
$\omega_{j,t}^{P,s}$	Forecasted active power output of renewable power generator *j* at time *t*.
u_{PV}	Associated coefficient for connecting active and reactive PV power.
$PF_{pv,min}$	Minimum power factor of PV system *pv*.
Q_{cb}^{cap}	Reactive power capability for capacitor bank *cb*.
V_0	Reference voltage magnitude.
$f_{l_e,max}^{a,}$, $f_{l_e,max}^{r,}$	Maximum active and reactive power flow of line l_e.
$P_{k_e,t}$, $Q_{k_e,t}, P_{k_g,t}$	Active and reactive power load and gas load at time *t*.

This work was supported by the National Natural Science Foundation of China (Nos. 72042018, 71621002).

P. Zhao and Z, Cao are with the Institute of Automation, Chinese Academy of Sciences, Beijing, China and School of Artificial Intelligence, University of Chinese Academy of Sciences, Beijing, China. (email: P. Zhao@bath.ac.uk, Zhidong.Cao@ia.ac.cn)

P. Zhao, C.Gu (corresponding author), Y. Bian and S. Li are with the Department of Electronic & Electrical Engineering, University of Bath, Bath, UK.(email: P. Zhao@bath.ac.uk; C.Gu@bath.ac.uk; Y. Bian@bath.ac.uk and S. Li@bath.ac.uk).

X. Lu is with the Department of Electrical Engineering, the Hong Kong Polytechnic University, Hong Kong (email: harry.lu@connect.polyu.hk)

Q. Ai is with the School of Electronic Information and Electrical Engineering Department of Electrical Engineering, Shanghai Jiao Tong University , Shanghai, China (e-mail: aiqian@sjtu.edu.cn).

H. Liu is with the School of Electrical and Information Engineering, Tianjin University, Tianjin, China. (email: liuhong@tju.edu.cn).

X. Chen is with the Electrical Engineering Department, Carnegie Mellon University, Pittsburgh, USA. (email: xinlei.chen@sv.cmu.edu)

$G_{i_g,max}$, $G_{i_g,min}$	Maximum and minimum output of natural gas source i_g.
$Pr_{l_g,max}$, $Pr_{l_g,m}$	Maximum and minimum gas pressure of gas pipeline l_g.
γ_{l_g}	Coefficient for Weymouth equation.
$f_{l_g,max}$	Maximum gas flow of pipeline l_g.
η_{GT}	Conversion efficiency of gas turbine.
Ω_{hy},Ω_{LPG}, Ω_{ni},Ω_{me}, Ω_{mix}	Gross calorific value (GCV) for hydrogen, liquid petroleum gas (LPG), nitrogen, methane and mixed natural gas.
ρ_{hy},ρ_{LPG},ρ_{ni} ,ρ_{me}	Gas density of hydrogen, liquid petroleum gas, nitrogen and methane.
E_{hy},E_{LPG},E_{ni} ,E_{me}	Combustion potential index (CPI) of hydrogen, liquid petroleum gas, nitrogen and methane.
O_i	Oxygen index.
Ω_{max}^{mix}, SG_{max}^{mix}, WI_{max}^{mix}, CP_{max}^{mix}	Maximum limit for GCV, specific gravity, wobbe index (WI) and Combustion Potential (CP) of mixed gas.
Ω_{min}^{mix}, SG_{min}^{mix}, WI_{min}^{mix}, CP_{min}^{mix}	Minimum limit for GCV, specific gravity (SG), WI and CP of mixed gas.
$\Delta\varphi_{n,max}^{hy\_me}$, $\Delta\varphi_{n,r}^{hy}$ $\Delta\varphi_{n,max}^{LPG}$, $\Delta\varphi_{n,m}^{ni}$ $\Delta\varphi_{n,max}^{me}$	Maximum volume deviation for hydrogen producing methane, direct used hydrogen, LPG, nitrogen and methane.
$\varphi_{n,max}^{mix}$, $\varphi_{n,min}^{mix}$	Maximum and minimum volume for mixed gas at node n.
Θ	Constant in Boyle's law.
$P_{k_e,max}^{ls}$ $P_{k_g,max}^{ls}$	Maximum power and gas load shedding at time *t*.
π_v	The penalty cost coefficient for penalizing the voltage deviation.
V_b^{ref}	Nominal voltage magnitude.
λ_N, λ_{LPG}	Cost coefficients for nitrogen and liquid petroleum gas.
λ_{sub}^a, λ_{sub}^r	Unit cost for active and reactive power supplied from upper market.
$\lambda_{i_e}^a$, $\lambda_{i_e}^b$, $\lambda_{i_e}^c$	Cost coefficients for generation of traditional DG i_e.
λ_{i_g}	Cost coefficient for generation of natural gas source i_g.
$\lambda_{i_e}^+$, $\lambda_{i_e}^-$	Cost coefficient for up and down reserve of traditional DG i_e.
$\lambda_{i_e}^{re}$, λ_j^{re}	Regulation cost coefficient for traditional DG i_e and renewable power generator j.
$\lambda_{k_e}^{ls}$, $\lambda_{k_g}^{ls}$	Penalty cost coefficient for power and gas load shedding.

In section *C*, the variables of both the first and second stages are represented. In the mathematical formulations, 'scheduled' and 'regulated' are represented by '*s*' and '*re*', indicating the decision variables at the first and second stages. Moreover, the 'initial' and 'terminal' for power buses and gas nodes are denoted as '*ini*' and '*ter*' as the superscripts.

D. Variables and functions

$P_{sub,t}$,$Q_{sub,t}$	Active and reactive power supply from upper market.
$r_{i_e,t}^+$, $r_{i_e,t}^-$, $r_{gt,t}^+$, $r_{gt,t}^-$	Up and down reserve capacity of generators and gas turbines.
$P_{i_e,t}$, $P_{gt,t}$	Output of traditional DGs and gas turbines.
$V_{b,t}$, $V_{sub,t}$	Voltage of bus *b* and substation at time *t*.
TP_t^{OLTC}	Tap position of OLTC at time *t*.
$\omega_{j,t}^Q$	Reactive power output of PV system *j* at time *t*.
$u_{cb,t}$, $Q_{cb,t}$	Switch status and output of capacitor bank *cb* at time *t*.
$V_{b,t}^{ini}$, $V_{b,t}^{ter}$	Voltage magnitude for initial and terminal nodes.
$f_{l_e,t}^a$, $f_{l_e,t}^r$	Active and reactive power flow at time *t*.
$G_{i_g,t}$	Output of natural gas sources.
$Pr_{n,t}$	Pressure of gas node *n*.
$f_{l_g,GT,t}$, $P_{gt,t}$	Injected gas flow and output of gas turbine.
$P_{n,t}^{P2G}$	Power consumed by the electrolyser.
$G_{n,t}^{hy}$, $G_{n,t}^{hy\_me}$, $G_{n,t}^{hy\_d}$, $G_{n,t}^{me}$	Gas output for overall P2G process, direct hydrogen injection, hydrogen during methanation process and methanation.
$G_{n,t}^{ca}$	Required gas of carbon dioxide during methanation process.
$\varphi_{n,t}^{hy\_me}$,$\varphi_{n,t}^{hy\_d}$ $\varphi_{n,t}^{LPG}$, $\varphi_{n,t}^{ni}$, $\varphi_{n,t}^{mix}$	Volume for hydrogen with methanation process, direct use, LPG, nitrogen, methane and mixed natural gas.
$\Omega_{n,t}^{mix}$, $SG_{n,t}^{mix}$, $WI_{n,t}^{mix}$, $CP_{n,t}^{mix}$	CGV, SG, WI and CP for mixed gas of node n at time *t*.
$P_{k_e,t}^{ls}$, $Q_{k_e,t}^{ls}$, $P_{k_g,t}^{ls}$	Power and gas load shedding at time *t*.

I. INTRODUCTION

In recent years, there is an increasing need for the integration of multi-energy vectors due to decarbonization and booming coupling technologies between energy infrastructures. Integrated energy system (IES) plays a vital part through coordinating energy supply, conversion, storage and consumption between each sub-system, e.g., power, gas, heat and cooling systems. The optimal operation of IES is one significant research topic, which ensures the economy and reliability of IES. Numerous studies in the existing literature have explored the optimal operation under renewable uncertainties [1-6].

To facilitate energy conversion and tighten system couplings, the emerging power-to-gas (P2G) has been recognized as an effective technique to convert surplus renewable energy into hydrogen, transported in natural gas systems. Considering the wide deployment of gas-fired generators, bidirectional energy flows between power and natural gas systems can be realized. Paper [1] proposes an optimal stochastic optimization (SO)-based P2G operation scheme in a day-ahead gas and power market to minimize gas storage operating expenditure. A coordination framework for maximizing the profit of wind farms with P2G facilities is proposed in [2]. The bidding strategy is modelled by a SO model with a cooperative game framework. Paper [7] designs a decentralized P2G operation scheme considering linearized transient-state gas flow. In general, inherent renewable uncertainty in IES impacts i) P2G conversion, ii) gas quality management, iii) voltage regulation, and iv) whole system operation.

Hydrogen can be injected into gas systems after being produced from P2G facilities. Consequently, the original gas composition would inevitably be changed due to hydrogen injection. The impact will further propagate to the gas system, affect the gas quality of end customers, and cause security problems [8]. Paper [9] proposes a simulation for the unsteady operation of natural gas systems with hydrogen injection. The risk assessment involves the change of gas composition, flow

rate and pressure profile, compared to the case without hydrogen injection. An assessment of the safety and working performance of gas appliances with the admixture of hydrogen is studied in [10]. In previous studies, the most common gas quality index to measure gas interchangeability is Wobbe index (WI). The influence of fuel variability on flame surface, flame normal and WI are investigated for hydrogen-enriched combustion in [11]. WI is used to measure the efficiency of combustion of syngas mixtures. Paper [12] utilizes WI as a pivotal standard to investigate the impact of WI on interoperability between different gas components. Gas interchangeability is studied in [10] based on WI, indicating that WI is highly associated with flashback issues and thus is essential to consider. To maximize the hydrogen production, the required level of WI and combustion potential (CP) for secure hydrogen operation is proposed in [13].

Although the interaction between each sub-system facilitates system economic performance and security, it also raises challenges to VVO as the system topology is changed and the bidirectional energy flow complicates the operation. Volt-Var-Optimization (VVO) is an essential requirement for distribution power systems to mitigate voltage deviations, reduce power losses and achieve reliable and economic system operation [14, 15]. VVO determines the optimal set of operation actions via voltage regulating devices, e.g., voltage regulators, on-load tap changers (OLTC), capacitor banks and renewable inverters [16]. Under the extensive renewable penetrated era, the rapidly growing penetration of renewable technologies will inevitably cause voltage fluctuations and affect the operations of voltage regulating devices. VVO models with optimal coordination of voltage regulating devices have been investigated widely in the existing literature and most papers consider renewable uncertainty for mitigating the resulted adverse impacts. Paper [17] deploys robust optimization (RO) to handle renewable uncertainty to ensure the economic coordination of all the devices, thus minimizing voltage deviations. The reformulated second-order cone programming model is solved by an improved column-and-constraint generation algorithm. Chance-constrained programming is utilized to model uncertain distributed generation and load demand simultaneously [18]. Paper [19] designs a game-theoretic VVO considering uncertain renewable generation, the mobility of electric vehicles and the demand response of microgrid customers. The uncertainties of renewable generation and mobility of electric vehicles are mitigated via setting short time slots.

The interdependencies in IES is enormous and the operation on a certain sub-system will propagate to other sub-systems. For instance, in an integrated electricity and gas system, the voltage regulation measures taken on the power system will influence the power and gas exchange, which eventually impacts the security and economic performance of the entire system. Moreover, gas systems can absorb surplus power generation via P2G facilities. Therefore, the study of VVO in IES is essential. The gas quality problem not only affects end customers but pressure scheduling and gas flow management of the gas system. The adjustment measures to maintain gas quality in the gas system then inevitably influences the VVO of the entire IES. An IES operator needs to ensure the secure, reliable and economic operation of electricity and gas systems. Therefore, gas quality and pressure management are regarded as equally significant as the VVO problem in the electricity system.

To capture renewable uncertainty, this paper applies the innovative two-stage distributionally robust optimization (DRO) to hedge against uncertain renewable fluctuations. As an alternative to traditional RO and SO, DRO provides more flexibility based on partial distribution information with a predetermined ambiguity set, which does not require the specific distribution assumption while mitigating the conservatism of RO [20-22]. Therefore, the impacts on VVO and P2G operation due to renewable uncertainties can be mitigated by using DRO. Here, PV uncertainty is handled by the moment-based ambiguity set in a two-stage framework, where the first stage provides the initial scheduling scheme based on predicted PV output and the second stage recourse decisions are determined when PV uncertainty is realized. Dual formulations are made for the original problem with the resulted semidefinite programming (SDP) reformulation with tractability, which can be solved efficiently by most current commercial solvers.

In summary, three main research problems and gaps in existing research are required to be resolved: i) P2G facilities can help absorb surplus renewable output with high fluctuation and mitigate voltage deviations, but has not been used yet; ii) gas quality issues due to hydrogen injection have not been considered in IES operation; and iii) VVO problem has been extensively studied in power systems whilst has never been investigated in IES with system interdependencies;

In this paper, a novel two-stage DRO for regulating voltage deviation, managing gas quality and guaranteeing optimal system operation is proposed in an IES. To mitigate voltage fluctuations, the optimal coordination of OLTCs, capacitor banks, PV systems and P2G facilities are used as voltage regulating measures. Gas quality is also ensured based on the proposed innovative gas quality and pressure management strategy, i.e., purchasing and mixing additional liquid petroleum gas (LPG) and nitrogen to maintain satisfactory gas quality indices. The proposed volt-VAR-pressure optimization is referred to as VVPO for simplicity. Comprehensive case studies are carried out to validate the effectiveness of the distributionally robust-VVPO (DR-VVPO) model.

The major contributions are as follows:

1) This paper is the first attempt to study the fundamental VVO problem in IES, considering energy interdependencies and couplings.
2) P2G facilities are considered for alleviating voltage deviations and PV fluctuation in addition to the traditional voltage regulating devices.
3) A gas quality management strategy is developed in the IES operation model, where gas pressure and quality indices are constrained within an acceptable range.
4) A two-stage DRO approach is used to handle PV uncertainties, which avoids assuming the explicit uncertainty distributions compared with SO-based VVO and mitigates the conservatism compared with RO-based VVO.

The rest of this paper is structured as follows. Section II describes gas quality indices and P2G modelling. Section III proposes the IES model. The ambiguity set of DRO is illustrated in section IV. Section V concludes the paper.

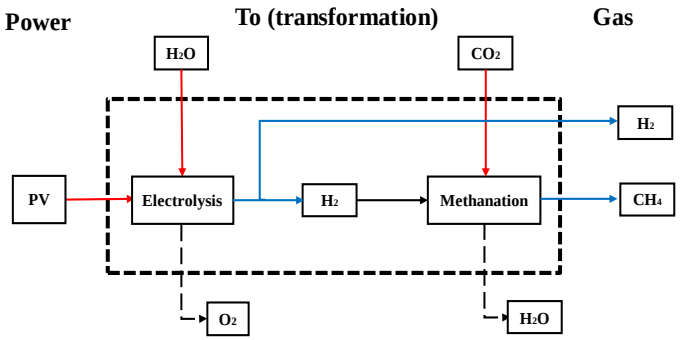

Fig. 1. The P2G process.

II. THE PROPOSED VVPO FRAMEWORK

A. Volt-VAR Optimziation Framework

As one of the fundamental functions in distribution systems, VVO maintains voltage profile within acceptable ranges, reduces power losses and ensures system economic operation. In this paper, VVO is achieved by determining the optimal set of controlling voltage regulating devices, e.g., OLTC, capacitor banks and PV regulation. The mathematical formulation of the proposed VVO framework is given as below. The voltage magnitude at each bus is constrained in (1). Equation (2) shows the expression of the voltage at the substation. Considering the wearing process of the transformer, the total number of OLTC operations is restricted in (3). Constraint (4) limits the PV reactive power support with the regulation coefficient defined in (5). The reactive power output of capacitor banks is shown in (6). And the linearized DistFlow equation for power flow in distribution systems is presented in (7). This equation is obtained based on the assumption that i) losses are negligible, ii) the voltage at each bus is close to 1.0 p.u. and iii) the voltage at the reference bus is 1.0 p.u. [23-25].

$$V_{b,min} \le V_{b,t} \le V_{b,max} \tag{1}$$

$$V_{sub,t} = V_{sub}^{ref} + \delta^{OLTC} TP_t^{s,OLTC} \tag{2}$$

$$\sum_{t\in T} \left| TP_t^{OLTC} - TP_{t-1,}^{OLTC} \right| \le nTP_{max}^{OLTC} \tag{3}$$

$$-u_{PV}\omega_{j,t}^{P} \le \omega_{j,t}^{Q} \le u_{PV}\omega_{j,t}^{P} \tag{4}$$

$$u_{PV} = \sqrt{\frac{1 - PF_{PV,min}{}^{2}}{PF_{PV,min}{}^{2}}} \tag{5}$$

$$Q_{cb,t} = u_{cb,t} Q_{cb}^{cap} \tag{6}$$

$$V_{b,t}^{ini} - V_{b,t}^{ter} = \left(f_{l_e,t}^{a} r_{l_e} + f_{l_e,t}^{r} x_{l_e}\right)/V_0 \tag{7}$$

B. Gas Quality Management

This paper ensures gas quality via four gas quality indices, i.e., WI, CP, specific gravity (SG) and gross calorific value (GCV). This section describes four indices and P2G modelling. The gas quality problems caused by the large variety are inevitable since i) many countries rely highly on gas imports and ii) different gas generation companies share the same gas transportation network. As the two most significant features for assessing the gas quality, gas adaptability and gas interchangeability are mostly employed for quality measurement. The gas adaptability is used to describe if the gas-fired appliances work under normal conditions with the variation of gas compositions. The gas interchangeability is used to describe the operational performance of gas facilities with regards to safety, emissions and efficiency. Overall, the variation of gas composition is permitted but it needs to be controlled within an acceptable range.

SG is described in (8) by the ratio of gas density over the air density [8, 26]. This paper applies SG to limit hydrocarbon content. The density of air, hydrogen and gas is denoted as ρ_{air}, ρ_{hy} and ρ_g, respectively. The hydrogen volume is represented by φ_{hy}. If the hydrocarbon content is at a relatively high amount, a series of combustion issues will be caused, e.g., more carbon monoxide emissions and spontaneous ignition events, etc.

Calorific value is used to define the amount of released heat during the gas combustion. In addition to that, GCV describes the amount of released heat when it is fully condensed and recovered, i.e., the gas temperature before and after the combustion is the same. GCV is required to restricted within a predetermined range. The expression of GCV of the mixed gas is given in (9) [27, 28], where the GCV value of gas and hydrogen are denoted as Ω_g and Ω_{hy} .

The measurement of gas combustion stability can be realized based on CP which characterizes the combustion features including flame issues and combustion flame and so forth. When the gases are interchangeable, the CP of each gas component should be close to each other. In (3), CP is defined, where the volume of hydrocarbon, carbon dioxide and methane are represented by φ_{cm}, φ_{hc} and φ_{me}, respectively [8, 13].

WI is a measure of interchangeability of gases that compares the combustion output of different gas components. Gas components are appropriate for a mixture when the WI of gases are close to identical. However, WI of each gas component is allowed to vary within 5-10%. If the variation is beyond the allowed range, the effects will be noticeable, e.g., high greenhouse gas emission and stability issues of gas equipment. Furthermore, the immediate WI variation will lead to emergency shutdowns of gas turbines, which has an adverse impact on the longevity of gas turbines. Equation (4) presents the expression of WI [29, 30].

P2G facilities enable to convert the abundant renewable generation to hydrogen. The process of the conversion via P2G is depicted in Fig. 1. In the first step, the electrolyser is applied to split water into hydrogen and oxygen powered by excessive renewable generation. Then methane is obtained with the addition of carbon dioxide in the methanation process. Meanwhile, the produced hydrogen can be directly injected into the gas system. The P2G output is given in (5). Equations (6)-(8) present methane production and the required amount of carbon dioxide according to Sabatier factors [31].

$$SG = \frac{\rho_g + \left(\rho_{hy} - \rho_g\right)\varphi_{hy}}{\rho_{air}} \tag{8}$$

$$\Omega = \Omega_g + \left(\Omega_{hy} - \Omega_g\right)\varphi_{hy} \tag{9}$$

$$CP = O_i \frac{\varphi_{hy} + 0.6(\varphi_{cm} + \varphi_{hc}) + 0.3\varphi_{me}}{\sqrt{SG}} \tag{10}$$

$$WI = \frac{\Omega}{\sqrt{SG}} \tag{11}$$

$$G_{n,t}^{hy} = \eta_e \frac{P_{n,t}^{P2G}}{\Omega_{hy}} \tag{12}$$

$$G_{n,t}^{hy\_me} + G_{n,t}^{hy\_d} = G_{n,t}^{hy} \tag{13}$$

$$G_{n,t}^{ca} = \eta_{hy-ca} G_{n,t}^{hy\_me} \tag{14}$$

$$G_{n,t}^{me} = \eta_{hy-me} G_{n,t}^{hy\_me} \tag{15}$$

III. System Modelling

In this paper, the two-stage DR-VVPO contains i) day-ahead voltage management involving maintaining voltage magnitude, determining optimal dispatch scheme of generators and ensuring satisfied gas quality and ii) real-time active adjustment based on the day-ahead optimization under the fluctuation of PV output. TABLE I summarizes all the decision variables with objectives and uncertainty treatment defined.

A. Day-Ahead Constraints of DR-VVPO

In the first stage, the day-ahead optimization is based on the forecasted renewable output before its uncertainty realised. Equations (1)-(7) and (16)-(39) are constraints of day-ahead DR-VVPO. The power purchase from the substation in the day-ahead upper-level energy market is limited in (16). For gas turbines and traditional DGs, the up and down reserve capacity is limited in (17) and (18). Constraints (19) and (20) regulates the output of traditional DGs and gas turbines. Constraint (21) limits the power flow magnitude. The balance constraints of active and reactive power are in (22) and (23).

In regards to the gas system, the constraints are shown in (5)-(8) and (24)-(39). The gas source output and pressure are limited in (24)-(26). Constraint (26) ensures the gas pressure at the initial gas nodes is higher than terminal nodes in the radial gas system. The gas flow is restricted between and upper and lower limits in (28). The output of the gas turbine is shown in (29). The theoretical constraints (1)-(4) are given as (30)-(33) under the real application. To guarantee the proposed gas quality indices are within the associated standard, constraint (34) is proposed. The deviation of the volume of each gas component between time slot *t*-1 and *t* is shown in (35) considering the normal gas transmitting speed in gas pipelines. The constraints of the total volume of all the gas components are shown in (36) and (37). Based on Boyle's law [32], the relationship between the gas volume and pressure are shown in (38). The last constraint (39) ensures the balancing condition in the gas system.

$$0 \le \{\cdot\}_{sub,t}^{s} \le \{\cdot\}_{sub,max}, \{\cdot\} = P, Q \tag{16}$$

$$0 \le r_{\{\cdot\},t}^{+} \le R_{\{\cdot\}}^{+}, \{\cdot\} = i_e, gt \tag{17}$$

$$0 \le r_{\{\cdot\},t}^{-} \le R_{\{\cdot\}}^{-}, \{\cdot\} = i_e, gt \tag{18}$$

$$P_{\{\cdot\},t}^{s} + r_{\{\cdot\},t}^{+} \le P_{\{\cdot\},max}, \{\cdot\} = i_e, gt \tag{19}$$

$$P_{\{\cdot\},min} \le P_{\{\cdot\},t}^{s} - r_{\{\cdot\},t}^{-}, \{\cdot\} = i_e, gt \tag{20}$$

$$0 \le f_{l_e,t}^{\{\cdot\},s} \le f_{l_e,max}^{\{\cdot\},s}, \{\cdot\} = a, r \tag{21}$$

$$\sum_{i_e \in I_e} P_{i_e,t}^{s} + \sum_{j \in J} \omega_{j,t}^{P,s} + \sum_{l_e \in L_e} f_{l_e,t}^{a,s,ini} - \sum_{l_e \in L_e} f_{l_e,t}^{a,s,ter} + \sum_{gt \in GT} P_{gt,t}^{s} = \sum_{k_e \in K_e} P_{k_e,t} + \sum_{n \in N} P_{n,t}^{s,P2G} \tag{22}$$

$$\sum_{i_e \in I_e} Q_{i_e,t}^{s} + \sum_{j \in J} \omega_{j,t}^{Q,s} + \sum_{cb \in CB} Q_{cb,t}^{s} + \sum_{l_e \in L_e} f_{l_e,t}^{r,s,ini} - \sum_{l_e \in L_e} f_{l_e,t}^{r,s,ter} = \sum_{k_e \in K_e} Q_{k_e,t} \tag{23}$$

$$G_{i_g,min} \le G_{i_g,t}^{s} \le G_{i_g,max} \tag{24}$$

$$Pr_{l_g,min}^{2} \le Pr_{l_g,t}^{s^2} \le Pr_{l_g,max}^{2} \tag{25}$$

$$Pr_{l_g,t}^{s,ini} \ge Pr_{l_g,t}^{s,ter} \tag{26}$$

$$f_{l_g,t}^{s\ 2} = \gamma_{l_g}\left(Pr_{l_g,t}^{s,ini^2} - Pr_{l_g,t}^{s,ter^2}\right) \tag{27}$$

$$0 \le f_{l_g,t}^{s} \le f_{l_g,max} \tag{28}$$

$$P_{gt,t}^{s} = c_{gt} f_{l_g,gt}^{s} \tag{29}$$

$$\Omega_{n,t}^{mix} = \Omega_{hy}\left(\varphi_{n,t}^{hy\_me} + \varphi_{n,t}^{hy\_d}\right) + \Omega_{LPG}\varphi_{n,t}^{LPG} + \Omega_{ni}\varphi_{n,t}^{ni} + \Omega_{me}\varphi_{n,t}^{me} \tag{30}$$

$$SG_{n,t}^{mix} = \left[\rho_{hy}\left(\varphi_{n,t}^{hy\_me} + \varphi_{n,t}^{hy\_d}\right) + \rho_{LPG}\varphi_{n,t}^{LPG} + \rho_{ni}\varphi_{n,t}^{ni} + \rho_{me}\varphi_{n,t}^{me}\right]\left(\varphi_{n,t}^{hy,me} + \varphi_{n,t}^{hy,d} + \varphi_{n,t}^{LPG} + \varphi_{n,t}^{ni} + \varphi_{n,t}^{me}\right) \tag{31}$$

$$WI_{n,t}^{mix} = \Omega_{n,t}^{mix} / \sqrt{SG_{n,t}^{mix}} \tag{32}$$

$$CP_{n,t}^{mix} = O_i \frac{E_{hy}\left(\varphi_{n,t}^{hy\_me} + \varphi_{n,t}^{hy\_d}\right) + E_{LPG}\varphi_{n,t}^{LPG} + E_{ni}\varphi_{n,t}^{ni} + E_{me}\varphi_{n,t}^{me}}{\sqrt{SG_{n,t}^{mix}}} \tag{33}$$

$$\{\cdot\}_{min} \le \{\cdot\} \le \{\cdot\}_{max}, \{\cdot\} = \Omega_{n,t}^{mix}, SG_{n,t}^{mix}, WI_{n,t}^{mix}, CP_{n,t}^{mix} \tag{34}$$

$$-\Delta\varphi_{n,max}^{\{\cdot\}} \le \varphi_{n,t}^{\{\cdot\}} - \varphi_{n,t-1}^{\{\cdot\}} \le \Delta\varphi_{n,max}^{\{\cdot\}}, \{\cdot\} = hy\_me, hy\_d, LPG, ni, me \tag{35}$$

$$\varphi_{n,t}^{hy,me} + \varphi_{n,t}^{hy,d} + \varphi_{n,t}^{LPG} + \varphi_{n,t}^{ni} + \varphi_{n,t}^{me} = \varphi_{n,t}^{mix} \tag{36}$$

$$\varphi_{n,min}^{mix} \le \varphi_{n,t}^{mix} \le \varphi_{n,max}^{mix} \tag{37}$$

$$\varphi_{n,t}^{mix} = \frac{\Theta}{Pr_{n,t}} \tag{38}$$

$$\sum_{i_g \in I_g} G_{i_g,t}^{s} + \sum_{n \in N} G_{n,t}^{s,hy} + \sum_{l_g \in L_g} f_{l_g,t}^{s,ini} - \sum_{l_g \in L_g} f_{l_g,t}^{s,ter} = \sum_{k_g \in K_g} G_{k_g,t} + \sum_{l_g \in L_g} f_{l_g,gt,t}^{s} \tag{39}$$

B. Real-Time Constraints of DR-VVPO

The real-time recourse VVPO can be implemented when the PV uncertainty is realized. The adjustment actions involve redispatching voltage regulating devices, traditional DGs and gas sources while providing the minimal load shedding schedule. In (40), the regulated output of generators is given. Constraint (41) limits both the power and gas load shedding. And the new balance constraints of power and gas systems are given in (42)-(44).

$$P_{\{\cdot\},t}^{re} - r_{\{\cdot\},t}^{-} \le P_{\{\cdot\},t}^{re} \le P_{\{\cdot\},t}^{re} + r_{\{\cdot\},t}^{+}, \{\cdot\} = i_e, gt \tag{40}$$

$$0 \le P_{\{\cdot\},t}^{ls} \le P_{\{\cdot\},max}^{ls}, \{\cdot\} = k_e, k_g \tag{41}$$

$$\sum_{i_e \in I_e} P_{i_e,t}^{re} + \sum_{j \in J} \xi_{j,t} + \sum_{gt \in GT} P_{gt,t}^{s} + \sum_{l_e \in L_e} f_{l_e,t}^{a,s,ini} - \sum_{l_e \in L_e} f_{l_e,t}^{a,s,ter} = \sum_{k_e \in K_e} P_{k_e,t} - P_{k_e,t}^{ls} + \sum_{n \in N} P_{n,t}^{re,P2G} \tag{42}$$

$$\sum_{i_e \in I_e} Q_{i_e,t}^{s} + \sum_{j \in J} \omega_{j,t}^{Q,s} + \sum_{cb \in CB} Q_{cb,t}^{s} + \sum_{l_e \in L_e} f_{l_e,t}^{r,s,ini} - \sum_{l_e \in L_e} f_{l_e,t}^{r,s,ter} = \sum_{k_e \in K_e} Q_{k_e,t} - Q_{k_e,t}^{ls} \tag{43}$$

TABLE I
TWO-STAGE VVPO FRAMEWORK

	Decision variables	Objective	Uncertainty treatment
Stage I	$P^s_{sub,t}, Q^s_{sub,t} P^s_{i_e,t}, r^+_{i_e,t}, r^-_{i_e,t}, r^+_{g,t}, r^-_{g,t}, V^s_{b,t}, V^s_{sub,t}, TP^{s,OLTC}_t$ $\omega^{Q,s}_{j,t}, u^s_{cb,t}, Q^s_{cb,t}, f^{a,s}_{l_e,t}, f^{r,s}_{l_e,t}, Pr^{s^2}_{l_g,t}, f^s_{l_g,t}, G^s_{l_g,t}, Pr^s_{l_g,t}, \varphi^{s,hy,me}_{n,t}$, $\varphi^{s,hy,d}_{n,t}, \varphi^{s,LPG}_{n,t}, \varphi^{s,ni}_{n,t}, \varphi^{s,me}_{n,t}, \Omega^{s,mix}_{n,t}, SG^{s,mix}_{n,t}, WI^{s,mix}_{n,t}, CP^{s,mix}_{n,t} \varphi^{s,mix}_{n,t}$	Voltage deviation, Generation and reserve cost for traditional DGs and natural gas sources, power purchase cost from upper market and voltage deviation penalty	Renewable generation forecast
Stage II	$P^{re}_{sub,t}, Q^{re}_{sub,t} P^{re}_{i_e,t}, V^{re}_{b,t}, V^{re}_{sub,t}, TP^{re,OLTC}_t \omega^{Q,re}_{j,t}, u^{re}_{cb,t}, Q^{re}_{cb,t}, f^{a,re}_{l_e,t}$ $f^{r,re}_{l_e,t}, Pr^{re^2}_{l_g,t}, f^{re}_{l_g,t}, G^s_{l_g,t}, Pr^s_{l_g,t}, \varphi^{s,hy,me}_{n,t}, \varphi^{s,hy,d}_{n,t}, \varphi^{s,LPG}_{n,t}, \varphi^{s,ni}_{n,t}, \varphi^{s,me}_{n,t}$ $\Omega^{s,mix}_{n,t}, SG^{s,mix}_{n,t}, WI^{s,mix}_{n,t}, CP^{s,mix}_{n,t} \varphi^{s,mix}_{n,t}$, $P^{ls}_{k_e,t}, P^{ls}_{k_g,t}$	Voltage deviation, Penalty cost for deviation of renewable, traditional DGs, natural gas sources, load shedding cost and voltage deviation penalty cost	Uncertain renewable generation, based on moment information

$$\sum_{i_g \in I_g} G^{re}_{i_g,t} + \sum_{l_g \in L_g} f^{re,ini}_{l_g,t} - \sum_{l_g \in L_g} f^{re,ter}_{l_g,t} = \sum_{k_g \in K_g} G_{k_g,t} - G^{ls}_{k_g,t} + \sum_{l_g \in L_g} f^{re}_{l_g,gt,t} \quad (44)$$

In addition to (40)-(44), the other constraints in the real-time stage are the same as the constraints of the first-stage when the superscript 's' is replaced by 're' due to the space limitation. Furthermore, the linearization is made for (16), (45) and (46), i.e., $\left|V^{\cdot}_{b,t} - V^{ref}_b\right|, \{\cdot\} = s, re$ and $\left|TP^{\cdot,OLTC}_t - TP^{\cdot,OLTC}_{t-1,}\right|, \{\cdot\} = s, re$ are linearized via incorporating new auxiliary variables (refs). And Mccormick inequality is used to relax constraints (17) and (19).

C. Objective Function of DR-VVPO

The first-stage objective aims to minimize the total voltage deviation at all buses over all the time periods and the operation cost, which is given in (45). The first term transforms the voltage deviation to the monetary objective when it is multiplied by the penalty coefficient. Noted that other than the hydrogen injection to the gas pipelines, the additional mixture of LPG and nitrogen is required to ensure the satisfied gas quality indices, which are shown in the second and third terms. The power purchase from the day-ahead upper market is given as the fourth term. The rest of (45) presents the generation cost and reserve cost of traditional DGs and gas sources.

$$\begin{aligned} \Gamma_1 = \min \sum_{i_e \in I_e, i_g \in I_g, t \in T} & \pi_v \left|V^s_{b,t} - V^{ref}_b\right| + \lambda^s_N \varphi^{s,ni}_{n,t} \\ & + \lambda^s_{LPG} \varphi^{s,LPG}_{n,t} + \lambda^a_{sub} P^s_{sub,t} + \lambda^a_{i_e} {P^s_{i_e,t}}^2 \\ & + \lambda^b_{i_e} P^s_{i_e,t} + \lambda^c_{i_e} + \lambda_{i_g} P^s_{i_g,t} + \lambda^+_{i_e} r^+_{i_e,t} \\ & + \lambda^-_{i_e} r^-_{i_e,t} \end{aligned} \quad (45)$$

Equation (46) illustrates the second-stage objective including i) economic loss caused by voltage deviation, ii) regulation cost of implementing gas quality management, iii) real-time power purchase from the upper power market, iv) the cost of redispatching traditional DGs and gas sources and v) the cost of load shedding of power and gas systems.

$$\begin{aligned} \Gamma_2 = \min \sum_{i_e \in I_e, i_g \in I_g, t \in T, k_e \in K_e, k_g \in K_g} & \pi_v \left|V^{re}_{b,t} - V^{ref}_b\right| \\ & + \lambda^{re}_N \left|\varphi^{re,ni}_{n,t} - \varphi^{s,ni}_{n,t}\right| \\ & + \lambda^{re}_{LPG} \left|\varphi^{re,LPG}_{n,t} - \varphi^{s,LPG}_{n,t}\right| \\ & + \lambda^a_{sub} P^{re}_{sub,t} + \lambda^{re}_j \left|\omega^s_{j,t} - \xi_{j,t}\right| \\ & + \lambda^{re}_{i_e} \left|P^s_{i_e,t} - P^{re}_{i_e,t}\right| + \lambda^{re}_{i_e} \left|P^s_{i_g,t} - P^{re}_{i_g,t}\right| \\ & + \lambda^{ls}_{k_e} P^{ls}_{k_e,t} + \lambda^{ls}_{k_g} P^{ls}_{k_g,t} \end{aligned} \quad (46)$$

IV. METHODOLOGY

In this section, the methodology for solving the DR-VVPO is given. To begin with, the original problem is presented via the abstract form of matrices and vectors. Then the ambiguity set construction for modelling the PV uncertainty is given. In the final step, dual reformulations are made. Noted that the DR-VVPO is a linear programming model. The integer variables, i.e., $TP^{re,OLTC}_t$ and $u^{re}_{cb,t}$ are relaxed as continuous variables.

A. Abstract Formulation

The compact form of the overall objective is given in (47) incorporating the first-stage and second-stage objective (45) and (46), which are represented by the first and second terms in (47), respectively. The constraints of the first and second stages are shown in (48) and (50).

$$\min_{x \in X} c'x + \sup_{Pf \in D} E_P[Q(x, \xi)] \quad (47)$$

$$\text{s.t. } Ax \le b, \quad (48)$$

$$Q(x, \xi) = \min_y f'y \quad (49)$$

$$\text{s.t. } Ex + Fy + G\xi \le h, \quad (50)$$

B. Constructing the Ambiguity Set

Instead of optimizing under a deterministic set via RO, the ambiguity set of DRO enables to model the uncertainty with a set of possible distributions. This paper employs the moment-based ambiguity set. The fixed mean vector and covariance matrix are employed to support the moment information. Rather than modelling an explicit distribution via SO, DRO enables to model a variety of distributions based on fixed moment information. In (58), the ambiguity set is given, which only utilizes moment information to model all the possible uncertainty distributions, e.g., Gaussian distribution, Weibull distribution, etc [21, 33]. The expressions in the proposed ambiguity set represent the integral of the probability distribution of ξ is 1 and all the probability distributions are based on the same mean vector and covariance matrix.

$$D = \left\{ f(\xi) \left| \begin{array}{c} \mathrm{P}\{\xi\} = 1 \\ \mathrm{E}\{\xi\} = \mu \\ \mathrm{E}\{\xi\,(\xi)'\} = \Sigma + \mu\,(\mu)' \end{array} \right. \right\} \quad (51)$$

C. Second-stage Dual Formulation

In the second-stage objective, the '*sup min*' framework needs to be reorganized as the dualized formulation with only '*min*'. Hence a dual formulation is required. Accordingly, the objective functions of the first and second stages can be merged.

Write $\sup_{Pf\in D} E_P[Q(x,\xi)]$ and (51) in its explicit form as (52)-(56) and $Pf(\xi)$ represents the probability density function.

$$S(x)^{primal} = \max_{Pf\in D_\xi} \int_\Xi Q(x,\xi)\, Pf(\xi) d\xi \quad (52)$$

$$\text{s.t. } Pf(\xi) \geq 0, \forall \xi \in \Xi \quad (53)$$

$$\int_\Xi Pf(\xi) d\xi = 1 \quad (54)$$

$$\int_\Xi \xi^m Pf(\xi) d\xi = \mu_m,\ m=1,2,\ldots,\Xi \quad (55)$$

$$\int_\Xi \xi^m \xi^n Pf(\xi) d\xi = \Sigma_{mn} + \mu_m \mu_n,\ m,\ n=1,2,\ldots,\Xi \quad (56)$$

The decision variable of (52)-(56) is $Pf(\xi)$ and there is an infinite number of variables given that the ambiguity set characterizes all the possible distributions. The dual reformulation is used to transform the infinite-dimensional primal form to a tractable dual form based on the strong duality theory [34]. The dual formulations are given in (57) and (58), which minimizes the dualized objective function based on the dual variables ψ_0, ψ_j and Ψ_{jk}.

Lemma: the results of (57) are equal to those of (52) with the strictly positive covariance matrix and strong duality ensured [35].

Consequently, the primal form is successfully transferred to the dual form. The infinite number of variables are transformed into a finite number of variables. Noted that Θ represents $\Sigma + \mu(\mu)'$ and the new compact form of DR-VVPO is given in (59).

$$S(x)^{dual} = \min_{\Psi,\psi,\psi_0} \langle \Psi'\Theta \rangle + \psi'\mu + \psi_0 \quad (57)$$

$$\text{s.t. } (\xi)'\Psi\xi + \psi'\xi + \psi_0 \geq Q(x,\xi), \forall \xi \in \Xi \quad (58)$$

$$\min_{x\in X} c'x + S(x)^{dual} \quad (59)$$

D. Semidefinite Programming

After the dual reformulation, equation (59) contains a finite number of variables while an infinite number of constraints. Thus, it is required with a further transformation into a closed form of $Q(x,\xi)$ to ensure computational tractability [36]. A new dual reformulation is made and given in (60) and (61) with the new dual variable τ, where VS is the polyhedral set accommodating extreme points. And the positive quadratic function is obtained as the new representation of (49), where N_v is the vertex set of the feasible region in VS.

$$\max_{u\in VS} \tau'(h - Ex - G\xi) \quad (60)$$

$$VS = \{\tau | F'\tau = f, \tau \leq 0\} \quad (61)$$

Equation (62) represents that the optimal solution of (49) can be determined from extreme points in VS. Equations (63) and (64) can be further obtained when (58) is substituted by (62).

$$\exists \tau \in VS: Q(x,\xi) = (h - Ex - G\xi)'\tau \quad (62)$$

$$(\xi)'\Psi\xi + \psi'\xi + \psi_0 \geq (h - Ex - G\xi)'\tau \quad \forall \xi \in \Xi,\ i=1,2,\ldots,N_v \quad (63)$$

$$(\xi)'\Psi\xi + (\psi + G'\tau^i)'\xi + \psi_0 - (h - Ex)\tau^i \geq 0 \quad \forall \xi \in \Xi,\ i=1,2,\ldots,N_v \quad (64)$$

The positive quadratic function (64) can be given as the compact matrix form in (65), which is an SDP problem. Compared with (59), tractability is ensured within a closed form.

$$\min_{x,\Psi,\psi,\psi_0} c'x + \langle \Psi'\Theta \rangle + \psi'\mu + \psi_0$$

$$\begin{bmatrix}\xi\\1\end{bmatrix}' \begin{bmatrix} \Psi & \frac{1}{2}(\psi + G'\tau^i) \\ \frac{1}{2}(\psi + G'\tau^i)' & \psi_0 - (h - Ex)'\tau^i \end{bmatrix} \begin{bmatrix}\xi\\1\end{bmatrix} \geq 0 \quad (65)$$

$$\forall \xi \in \Xi,\ i=1,2,\ldots,N_v,\ x \in X, \forall \tau^i \in VS$$

V. Case Studies

This section illustrates the effectiveness of the proposed DR-VVPO through 8 cases as shown in TABLE II. Cases 1 and 2 are used to compare the computational performance between RO and DRO. Cases 3-5 are used to show the impact of the gas system on voltage regulation. The impact of the capacity of regulating devices on voltage regulation is investigated among comparison between cases 2, 6 and 7. Case 8 is used to show the impact of gas quality management on DR-VVPO. A 33-bus20-node IES is shown in Fig. 2, with 3 traditional DGs, 4 PV systems and 7 capacitor banks connected [37]. The capacity for each capacitor bank and PV system are 400kVar and 360kVA, respectively. The interdependent power and gas systems are connected by three P2G facilities and two gas turbines. In TABLEs III and IV, the parameters of natural gas sources and traditional DGs are given. The GCV and combustion potential index (CPI) for hydrogen, methane, LPG and nitrogen are given in TABLE V. The gas composition of original natural gas and LPG is provided in TABLE VI, mainly consisting of methane, ethane, propane and butane. LPG has high GCV but low CPI, which is used to increase WI and decrease CP. By contrast, the GCV and CPI of nitrogen are both zero, which enables a more flexible gas mixture.

A. Studies on Voltage Management

The voltage profiles for cases 2-5 are over all the periods are given in Fig. 3. The mean voltage profile over 24 hours is shown as the red dotted curve. For all the cases, the voltage magnitude drops from bus 1 to 18. Since the supply decreases at the same branch when it approaches the loads at the branch end. Then the voltage magnitude respectively from bus 18 to 20 and followed by the approximately decrease until bus 33. In case 2, besides the voltage at the main branch, i.e., buses 1-18, the voltage profile at buses 19, 23 and 26 are relatively higher than other buses. Cases 2 and 3 show similar voltage profile, i.e., ranging from 0.97 p.u. to 1.02 p.u.. The distinct difference can be found between bus 15-19. The voltage magnitude of case 3 is lower than those of case 2. The reason is that there is no gas-to-power (G2P) in case 3, which fails to supply extra support from the gas system. However, case 2 has two connections of G2P at buses 15 and 19. As for case 4, P2G facilities are not considered in the system topology. The obtained voltage profile is obviously different compared with cases 2 and 3. The voltage magnitude ranges between 0.97 p.u. and 1.03 p.u.. This case implies that P2G is effective for mitigating the voltage fluctuation via absorbing excessive PV generation. The distinct voltage profile differences are between buses 1-5 and buses 19-25. The power and gas systems are disconnected in case 5 and the voltage fluctuation is higher than that of cases 2 and 3, which ranges from 0.97 p.u. to 1.05 p.u..

The scheduling of OLTC tap positions for cases 2, 5-7 is given in Fig. 4. Case 5 results in the highest tap positions among the four considered cases. The reason is that without P2G connections, the fluctuation of PV systems causes higher power

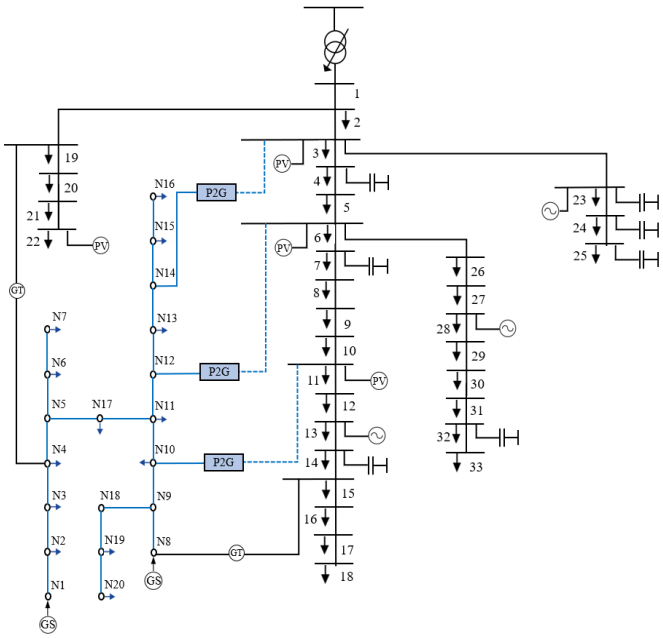

Fig. 2. The proposed 33-bus-20-node IES.

TABLE II
CASE ILLUSTRATION

Case No.	Optimization method	Capacitor bank capacity (kVar)	PV system capacity (kVA)	Gas system connection	Gas quality management
1	Robust	360	400	Yes	Yes
2	DRO	360	400	Yes	Yes
3	DRO	360	400	P2G	Yes
4	DRO	360	400	G2P	Yes
5	DRO	360	400	No	Yes
6	DRO	720	400	Yes	Yes
7	DRO	360	800	Yes	Yes
8	DRO	360	400	Yes	No

TABLE III
PARAMETERS OF NATURAL GAS SOURCES

Node No.	$P_{i_g,min}$ (kcf/h)	$P_{i_g,max}$ (kcf/h)	λ_{i_g} ($/kcf)
1	1000	6000	2.2
8	1000	3000	2

TABLE IV
GENERATOR PARAMETERS

Bus No.	$P_{i_e,max}$ (MW)	$P_{i_e,min}$ (MW)	$R^+_{i_e}, R^-_{i_e}$ (MW)	$\lambda^a_{i_e}$ ($/MW)	$\lambda^b_{i_e}$ ($/MW)	$\lambda^c_{i_e}$ ($)
13	1.2	0.3	0.2	6000	7100	6200
23	1.2	0.3	0.2	4500	10500	4000
28	1.0	0.1	0.2	4500	10500	4000

TABLE V
GCV AND CPI FOR DIFFERENT GASES

	H_2	CH_4	LPG	N_2
GCV	10	40	115	0
CPI	100	50	42	0

TABLE VI
GAS COMPOSITION (%)

	CH_4	C_2H_6	C_3H_8	C_4H_{10}	CO_2	*Other*
Natura gas	79.6	8.3	4.9	1.4	3.4	2.4
LPG	91.1	4.3	3.0	1.4	0	0.2

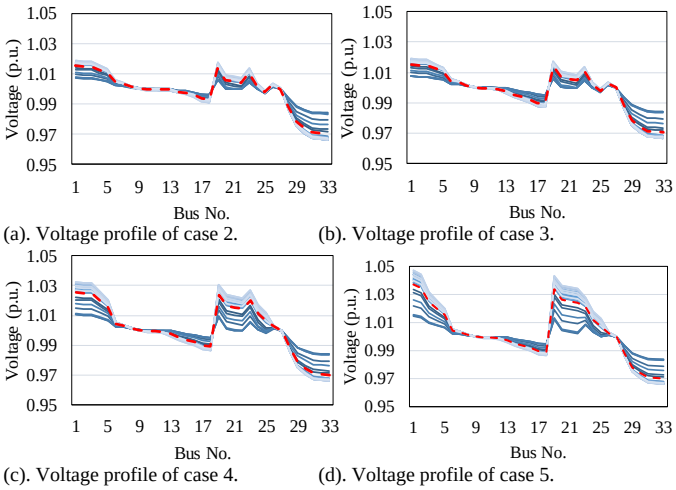

Fig. 3. Expected real-time voltage profiles for cases 2, 3, 4 and 5.

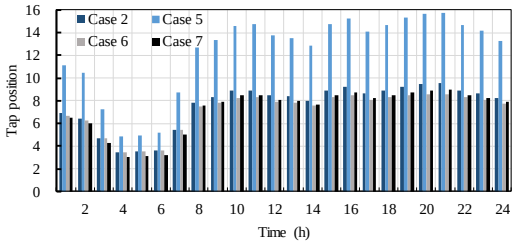

Fig. 4. OLTC tap position for cases 2, 5, 6 and 7.

flow and thus affect the high voltage issues. The tap position decreases from +11 to +5 between 1:00 and 4:00. It rises after 7:00, followed by a fluctuation afterwards. It peaks at +16 at 20:00 during the peak-load time period, which also witnesses the highest tap position of other cases. Cases 2, 6 and 7 show similar tap profile, which indicates that the additional capacity of capacitor banks and PV systems result in lower impact compared with employing P2G facilities.

B. Studies on Economic Performance

In TABLE VII, the operation cost for both the first and second stages are shown. Case 5 yields the highest operation cost at the two stages, i.e., $502542 and $127567. The reason is that case 5 is studied in a pure power system without any cost-effective supply from gas sources. In comparison, the total operation cost of case 8 is the lowest, $474967, which is only 75% of case 5. The reason is that gas quality management is not conducted which avoids the high purchase cost of LPG and nitrogen to maintain the permitted gas quality. Cases 1 and 2 deal with the PV uncertainty via RO and DRO, respectively. The single-stage RO provides a higher total operation cost ($548440) than that of DRO ($546692). And even the single-stage operation cost is higher than the sum of the cost of first and second stages via DRO. This proves the over-conservatism of RO as it considers the worst-case of PV output. The two-stage DRO mitigates the conservatism by providing a '*here-and-now*' and '*wait-and-see*' hierarchical framework with flexibility on dispatch adjustment and incorporates the distribution information in the ambiguity set. Cases 3 and 4 consider a single connection between power and gas systems. The results show that case 4 yields a higher cost than that of

TABLE VII
ECONOMIC PERFORMANCE FOR CASES 1-8

Economic result	Case 1	Case 2	Case 3	Case 4
First-stage cost ($)	548440	481711	495904	497171
Expected Second-stage cost ($)	0	64981	65325	122795
Total cost ($)	548440	546692	561229	619967
Economic result	**Case 5**	**Case 6**	**Case 7**	**Case 8**
First-stage cost ($)	502542	478013	476511	421013
Expected Second-stage cost ($)	127567	64390	63886	53954
Total cost ($)	630109	542403	540396	474967

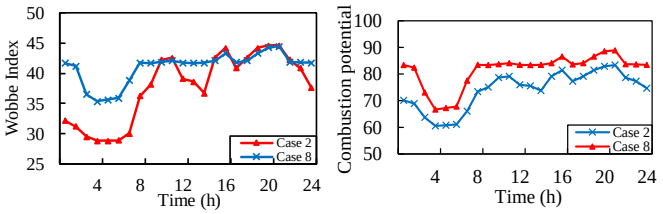

(a). Wobbe index. (b). Combustion potential.

Fig. 5. Gas quality indices for cases 2 and 8.

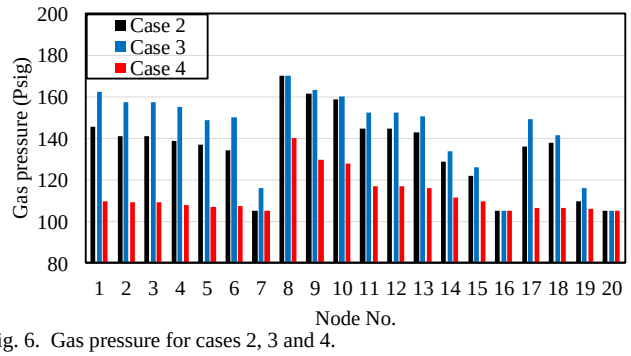

Fig. 6. Gas pressure for cases 2, 3 and 4.

case 3, which implies that the three P2G facilities are essential for improving the economic efficiency by transforming the surplus PV generation to gas loads. Compared with case 2, cases 3 and 4 have lower operation cost, which indicates the advantages of coordination and complementation of IES on system economic efficiency compared with the single operating power system. Cases 6 and 7 result in lower operating cost compared with case 2 due to their larger capacity of PV systems and capacitor banks.

C. *Studies on Gas Quality Management*

The gas quality management strategy of VVPO is proposed in this subsection, considering four quality indices and the gas pressure variation at each node. Fig. 5 depicts the variation of gas quality indices at node 10. The comparison is made between the benchmark case 2 and case 8 without gas quality management considered. Overall, case 2 shows higher WI compared with case 8. But the CP of case 2 shows lower results than case 8. It is to be noted that the permitted WI range is between 35 and 50. However, case 8 results in WI that is lower than the lower limit before 8:00. The low WI will lead to ignition problems, i.e., more gas amount is required for ignition

TABLE VIII
CASE ILLUSTRATION

Case No.	Capacitor bank capacity (kVA)	PV system capacity (kVA)	Gas system connection
1	360	800	Two
2	720	800	Two
3	360	1600	Two
4	360	800	No

TABLE IX
COST OF EACH STAGE

Economic result	Case 1	Case 2	Case 3	Case 4
First-stage cost ($)	47274	46052	42723	51868
Expected Second-stage cost ($)	3190	3074	3055	4012
Total cost ($)	50464	49126	45778	55880

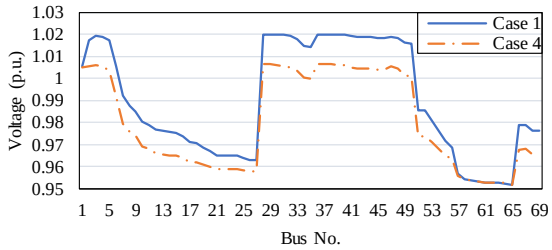

Fig. 7. Expected real-time voltage profile s for cases 1 and 4.

on the same gas equipment. Meanwhile, an unstable flame will be possibly caused. The CP is given in Fig. 5 (b), which shows that the CP if case 8 is higher than case 2 which shows that the hydrogen amount of case 8 is more than that of case 2. However, this is dangerous as inefficient combustion and even gas explosion might occur. In Fig. 6, the gas pressure is scheduled based on the optimal gas quality management. Cases 2-4 are studied with different system interconnections. The pressures at nodes 1 and 8 are higher than that of other nodes because of the direct connection of natural gas sources. The pressure decreases along the direction of gas flow. Nevertheless, another pressure peak occurs at gas node 17 when the gas flow from the two branches gather and supply node 17. Case 3 presents the highest pressure at all nodes compared with cases 2 and 4. Since the single connection from power to the gas system provides additional supply via P2G facilities.

D. *Scalability Analysis*

The scalability study is conducted in a 69-bus-20-node IES. There are 6 PV systems connected at buses 9, 23, 26, 34, 44 and 58, respectively. The 12 capacitor banks and transformer are used to compensate the reactive power. The 20-node gas system contains two natural gas sources and two gas turbines, which are connected between the gas and power systems. The data can be found in [37]. This section considers 4 cases which are shown in TABLE VIII.

As given in TABLE IX, case 4 has the highest total cost while case 3 has the lowest total cost. Compared with the benchmark case, i.e, case 1, there is no connection between electricity and gas systems in case 4. The capacity of capacitor banks and PV

systems are twice as case 1 in cases 2 and 3, yielding $1338 and $4686 less operation cost.

In Fig. 7, the voltage profiles of cases 1 and 2 are studied to investigate the impact from gas system connection. In case 1, it can be seen that the voltage level is decreasing along the main branch from bus 5 to bus 28. And the voltage level remains approximately the same value between bus 28 and bus 50 at 1.02 p.u.. With two gas turbines connected, the voltage level ranges from 0.952 p.u. to 1.020 p.u.. With only one connection with the gas system, the voltage level is lower than that of case 1, which ranges from 0.952 p.u. to 1.007 p.u.. Compared with case 1, when no gas turbines equipped, the voltage profile decreases by 0.8% in case 2. The comparison between cases 1 and 2 shows the increase of the voltage level for all buses with the addition of gas system connection.

E. Discussion on the Results

This section summarizes the results obtained from the extensive case studies in section V. The economic studies on 8 cases in 33-bus-20-node and 69-bus-20-node IESs indicate that
i) DRO is effective on mitigating the conservatism of RO;
ii) The doubled PV capacity is effective for reducing the overall operation cost.
iii) Omitting the gas quality management will effectively decrease the operation cost.

The voltage profile results show that the gas system enables to address the voltage fluctuation through offsetting the surplus power generation. Moreover, the traditional voltage regulating devices, i.e., PV systems, OLTC and capacitor banks also provide effective voltage regulation measures. However, the proposed gas quality management has a minor impact on VVO. The results of the gas quality indices and gas pressure study show that without the gas quality management, the proposed 4 gas quality indices are violated. Accordingly, the joint optimization of VVO and gas pressure is highly essential for ensuring both voltage profiles and high-quality gas supply.

The total computation time is approximately two hours, where the first-stage problem takes most of the time since the vertex set is extremely vast and the approach to find the optimality is time-consuming. However, when O^* and x^* are obtained, the real-time stage only takes averagely 30 seconds with 1000 simulation samples. Thus, the computational time of the real-time stage is acceptable in practice.

In addition to the proposed VVPO model, Volt-VAR-droop control (VVDC) has been designed for local voltage regulations to obtain stable frequency. Existing papers have extensively investigated VVDC models considering uncertainties based on data-driven scenario approaches or robust control [14,15]. However, VVDC is not viable to be resolved by DRO at present, as DRO requires fully linearized and static mathematical formulations. Currently, stochastic or robust approaches are more practical to solve VVDC. And the distributionally robust control model is out of the scope of this paper.

There are many remaining challenges in the current VVPO model and four major ones are as follows:

- Various energy storage systems in IES, including battery, gas and hydrogen, which be incorporated into the VVPO model for helping voltage regulations.
- It will investigate the volt-VAR control and the feasibility of combining it with the proposed two-stage DRO approach.
- Gas quality management may cause congestion issues for gas pipelines due to the admixture of hydrogen, nitrogen and LPG. Therefore, gas pipeline congestion will be considered and managed.
- Uncertain PV fluctuations could occur at the minute level. Therefore, a multi-timescale VVPO model containing finer temporal resolution will be investigated, particularly combined with the DRO approach.

VI. CONCLUSION

A two-stage VVPO model is developed to regulate voltage deviation, manage gas quality and minimize system operation cost of IES. Emerging P2G facilities are applied for voltage regulation via transferring excessive PV energy to hydrogen and transported in the gas system. The novel gas quality management is proposed for satisfying gas quality standards. The two-stage DRO is utilized to capture PV uncertainty and the reformulated SDP problem is solved efficiently by CGA. Some key findings are given:

- P2G facilities effectively contribute to voltage management.
- A secure IES operation is realized based on the proposed gas quality management strategy.
- Compared to the pure power system, the system operation cost in IES with interconnections is reduced greatly.
- The optimal coordination of energy conversion technologies enables to improve the energy utilization efficiency.

The proposed DR-VVPO presents a practical operation scheme for system operators for ensuring the voltage profile security and gas quality with lower operation cost under the multi-energy and high renewable integration era.

REFERENCES

[1] F. Liu, Z. Bie, and X. Wang, "Day-Ahead Dispatch of Integrated Electricity and Natural Gas System Considering Reserve Scheduling and Renewable Uncertainties," *IEEE Transactions on Sustainable Energy*, vol. 10, no. 2, pp. 646-658, 2019, doi: 10.1109/TSTE.2018.2843121.

[2] R. Zhang, T. Jiang, F. F. Li, G. Li, H. Chen, and X. Li, "Coordinated Bidding Strategy of Wind Farms and Power-to-Gas Facilities using a Cooperative Game Approach," *IEEE Transactions on Sustainable Energy*, pp. 1-1, 2020, doi: 10.1109/TSTE.2020.2965521.

[3] X. Xu, Y. Jia, Y. Xu, Z. Xu, S. Chai, and C. S. Lai, "A Multi-agent Reinforcement Learning based Data-driven Method for Home Energy Management," *IEEE Transactions on Smart Grid*, pp. 1-1, 2020, doi: 10.1109/TSG.2020.2971427.

[4] P. Zhao, C. Gu, Z. Hu, X. I. E. D, I. Hernando-Gil, and Y. Shen, "Distributionally Robust Hydrogen Optimization with Ensured Security and Multi-Energy Couplings," *IEEE Transactions on Power Systems*, pp. 1-1, 2020, doi: 10.1109/TPWRS.2020.3005991.

[5] S. Li, H. He, C. Su, and P. Zhao, "Data driven battery modeling and management method with aging phenomenon considered," *Applied Energy*, vol. 275, p. 115340, 2020/10/01/ 2020, doi: https://doi.org/10.1016/j.apenergy.2020.115340.

[6] S. Li, H. He, and J. Li, "Big data driven lithium-ion battery modeling method based on SDAE-ELM algorithm and data pre-processing technology," *Applied Energy*, vol. 242, pp. 1259-1273, 2019/05/15/ 2019, doi: https://doi.org/10.1016/j.apenergy.2019.03.154.

[7] F. Qi, M. Shahidehpour, F. Wen, Z. Li, Y. He, and M. Yan, "Decentralized Privacy-Preserving Operation of Multi-Area Integrated Electricity and Natural Gas Systems with Renewable Energy Resources," *IEEE Transactions on Sustainable Energy*, pp. 1-1, 2019, doi: 10.1109/TSTE.2019.2940624.

[8] I. Union, "Petroleum B. guidebook to gas interchangeability and gas quality," 2011.

[9] G. Guandalini, P. Colbertaldo, and S. Campanari, "Dynamic modeling of natural gas quality within transport pipelines in presence of hydrogen injections," *Applied Energy*, vol. 185, pp. 1712-1723, 2017/01/01/ 2017, doi: https://doi.org/10.1016/j.apenergy.2016.03.006.
[10] H. de Vries, A. V. Mokhov, and H. B. Levinsky, "The impact of natural gas/hydrogen mixtures on the performance of end-use equipment: Interchangeability analysis for domestic appliances," *Applied Energy*, vol. 208, pp. 1007-1019, 2017/12/15/ 2017, doi: https://doi.org/10.1016/j.apenergy.2017.09.049.
[11] K. K. J. Ranga Dinesh, X. Jiang, and J. A. van Oijen, "Hydrogen-enriched non-premixed jet flames: Analysis of the flame surface, flame normal, flame index and Wobbe index," *International Journal of Hydrogen Energy*, vol. 39, no. 12, pp. 6753-6763, 2014/04/15/ 2014, doi: https://doi.org/10.1016/j.ijhydene.2014.01.208.
[12] J. L. Zachariah-Wolff, T. M. Egyedi, and K. Hemmes, "From natural gas to hydrogen via the Wobbe index: The role of standardized gateways in sustainable infrastructure transitions," *International Journal of Hydrogen Energy*, vol. 32, no. 9, pp. 1235-1245, 2007/06/01/ 2007, doi: https://doi.org/10.1016/j.ijhydene.2006.07.024.
[13] C. Gu, C. Tang, Y. Xiang, and D. Xie, "Power-to-gas management using robust optimisation in integrated energy systems," *Applied Energy*, vol. 236, pp. 681-689, 2019/02/15/ 2019, doi: https://doi.org/10.1016/j.apenergy.2018.12.028.
[14] A. Singhal, V. Ajjarapu, J. Fuller, and J. Hansen, "Real-Time Local Volt/Var Control Under External Disturbances With High PV Penetration," *IEEE Transactions on Smart Grid*, vol. 10, no. 4, pp. 3849-3859, 2019, doi: 10.1109/TSG.2018.2840965.
[15] H. Zhu and H. J. Liu, "Fast Local Voltage Control Under Limited Reactive Power: Optimality and Stability Analysis," *IEEE Transactions on Power Systems*, vol. 31, no. 5, pp. 3794-3803, 2016, doi: 10.1109/TPWRS.2015.2504419.
[16] Y. Xu, Z. Y. Dong, R. Zhang, and D. J. Hill, "Multi-Timescale Coordinated Voltage/Var Control of High Renewable-Penetrated Distribution Systems," *IEEE Transactions on Power Systems*, vol. 32, no. 6, pp. 4398-4408, 2017, doi: 10.1109/TPWRS.2017.2669343.
[17] T. Ding, S. Liu, W. Yuan, Z. Bie, and B. Zeng, "A Two-Stage Robust Reactive Power Optimization Considering Uncertain Wind Power Integration in Active Distribution Networks," *IEEE Transactions on Sustainable Energy*, vol. 7, no. 1, pp. 301-311, 2016, doi: 10.1109/TSTE.2015.2494587.
[18] F. U. Nazir, B. C. Pal, and R. A. Jabr, "A Two-Stage Chance Constrained Volt/Var Control Scheme for Active Distribution Networks With Nodal Power Uncertainties," *IEEE Transactions on Power Systems*, vol. 34, no. 1, pp. 314-325, 2019, doi: 10.1109/TPWRS.2018.2859759.
[19] M. H. K. Tushar and C. Assi, "Volt-VAR Control Through Joint Optimization of Capacitor Bank Switching, Renewable Energy, and Home Appliances," *IEEE Transactions on Smart Grid*, vol. 9, no. 5, pp. 4077-4086, 2018, doi: 10.1109/TSG.2017.2648509.
[20] P. Zhao, C. Gu, D. Huo, Y. Shen, and I. Hernando-Gil, "Two-Stage Distributionally Robust Optimization for Energy Hub Systems," *IEEE Transactions on Industrial Informatics*, vol. 16, no. 5, pp. 3460-3469, 2020, doi: 10.1109/TII.2019.2938444.
[21] X. Lu, K. W. Chan, S. Xia, X. Zhang, G. Wang, and F. Li, "A Model to Mitigate Forecast Uncertainties in Distribution Systems Using the Temporal Flexibility of EVAs," *IEEE Transactions on Power Systems*, vol. 35, no. 3, pp. 2212-2221, 2020, doi: 10.1109/TPWRS.2019.2951108.
[22] P. Zhao, C. Gu, and D. Huo, "Two-Stage Coordinated Risk Mitigation Strategy for Integrated Electricity and Gas Systems under Malicious False Data Injections," *IEEE Transactions on Power Systems*, pp. 1-1, 2020, doi: 10.1109/TPWRS.2020.2986455.
[23] H. Yeh, D. F. Gayme, and S. H. Low, "Adaptive VAR Control for Distribution Circuits With Photovoltaic Generators," *IEEE Transactions on Power Systems*, vol. 27, no. 3, pp. 1656-1663, 2012, doi: 10.1109/TPWRS.2012.2183151.
[24] B. Wang, C. Zhang, and Z. Dong, "Interval Optimization Based Coordination of Demand Response and Battery Energy Storage System Considering SoC Management in A Microgrid," *IEEE Transactions on Sustainable Energy*, pp. 1-1, 2020, doi: 10.1109/TSTE.2020.2982205.
[25] S. Doan, H. Yeh, and Y. Yang, "Two-Mode Adaptive Schemes for VAR Control With Solar Power and Energy Storage," *IEEE Systems Journal*, vol. 14, no. 1, pp. 889-899, 2020, doi: 10.1109/JSYST.2019.2920016.
[26] P. S. Roy, C. Ryu, and C. S. Park, "Predicting Wobbe Index and methane number of a renewable natural gas by the measurement of simple physical properties," *Fuel*, vol. 224, pp. 121-127, 2018/07/15/ 2018, doi: https://doi.org/10.1016/j.fuel.2018.03.074.
[27] Z. Hu and X. Zhang, "Study on laminar combustion characteristic of low calorific value gas blended with hydrogen in a constant volume combustion bomb," *International Journal of Hydrogen Energy*, vol. 44, no. 1, pp. 487-493, 2019/01/01/ 2019, doi: https://doi.org/10.1016/j.ijhydene.2018.02.055.
[28] L. Kong, L. Su, X. Zhou, L. Chen, and Q. Liu, "Accuracy guarantee for determining the calorific value for dual gas sources," *Flow Measurement and Instrumentation*, vol. 65, pp. 233-239, 2019/03/01/ 2019, doi: https://doi.org/10.1016/j.flowmeasinst.2019.01.003.
[29] M. Deymi-Dashtebayaz, A. Ebrahimi-Moghadam, S. I. Pishbin, and M. Pourramezan, "Investigating the effect of hydrogen injection on natural gas thermo-physical properties with various compositions," *Energy*, vol. 167, pp. 235-245, 2019/01/15/ 2019, doi: https://doi.org/10.1016/j.energy.2018.10.186.
[30] L. Xiang, G. Theotokatos, and Y. Ding, "Investigation on gaseous fuels interchangeability with an extended zero-dimensional engine model," *Energy Conversion and Management*, vol. 183, pp. 500-514, 2019/03/01/ 2019, doi: https://doi.org/10.1016/j.enconman.2019.01.013.
[31] C. Toro and E. Sciubba, "Sabatier based power-to-gas system: Heat exchange network design and thermoeconomic analysis," *Applied Energy*, vol. 229, pp. 1181-1190, 2018/11/01/ 2018, doi: https://doi.org/10.1016/j.apenergy.2018.08.036.
[32] J. Qiu, J. Zhao, H. Yang, D. Wang, and Z. Y. Dong, "Planning of solar photovoltaics, battery energy storage system and gas micro turbine for coupled micro energy grids," *Applied Energy*, vol. 219, pp. 361-369, 2018/06/01/ 2018, doi: https://doi.org/10.1016/j.apenergy.2017.09.066.
[33] X. Lu, K. W. Chan, S. Xia, B. Zhou, and X. Luo, "Security-Constrained Multiperiod Economic Dispatch With Renewable Energy Utilizing Distributionally Robust Optimization," *IEEE Transactions on Sustainable Energy*, vol. 10, no. 2, pp. 768-779, 2019, doi: 10.1109/TSTE.2018.2847419.
[34] E. Delage and Y. Ye, "Distributionally robust optimization under moment uncertainty with application to data-driven problems," *Operations research*, vol. 58, no. 3, pp. 595-612, 2010.
[35] D. Bertsimas, X. V. Doan, K. Natarajan, and C.-P. Teo, "Models for minimax stochastic linear optimization problems with risk aversion," *Mathematics of Operations Research*, vol. 35, no. 3, pp. 580-602, 2010.
[36] Y. Chen, W. Wei, F. Liu, and S. Mei, "Distributionally robust hydro-thermal-wind economic dispatch," *Applied Energy*, vol. 173, pp. 511-519, 2016/07/01/ 2016, doi: https://doi.org/10.1016/j.apenergy.2016.04.060.
[37] I. I. o. T. Electrical and Computer Engineering Department. "Index of /data." motor.ece.iit.edu/data/ (accessed.

Pengfei Zhao (S'18) was born in Beijing, China. He received the double B.Eng. degree from the University of Bath, U.K., and North China Electric Power University, Baoding, China, in 2017. He is currently pursuing the Ph.D. degree with the Department of Electronic and Electrical Engineering, University of Bath, U.K. He was a visiting Ph.D. student at Smart Grid Operations and Optimization Laboratory (SGOOL), Tsinghua University, Beijing, China in 2019. His major research interests include the operation and planning of integrated energy systems considering inherent uncertainties.

Xi Lu received the B.Eng. degree in Electrical Engineering from North China Electric Power University, Beijing, China in 2015. He is currently pursuing the PhD degree in Electrical Engineering at the Hong Kong Polytechnic University, Hong Kong, China. His research interests include dispatch of electric vehicle aggregators, distribution system operation and applications of robust optimization and distributionally robust optimization in power systems, etc.

Chenghong Gu (M'14) was born in Anhui province, China. He received the Master's degree from the Shanghai Jiao Tong University, Shanghai, China, in 2007 in electrical engineering. He received the Ph.D. degree from the University of Bath, U.K. He is currently a Lecturer and EPSRC Fellow with the Department of Electronic and Electrical Engineering, University of Bath. His major research interest is in multi-vector energy system, smart grid, and power economics.

Qian Ai (Senior Member, IEEE) received the bachelor's degree in electrical engineering from Shanghai Jiao Tong University, Shanghai, China, in 1991, the master's degree in electrical engineering from Wuhan University, Wuhan, China, in 1994, and the Ph.D. degree in electrical engineering from Tsinghua University, Beijing, China, in 1999. He was with Nanyang Technological University, Singapore, for one year and the University of Bath, Bath, U.K., for two years. He was with Shanghai Jiao Tong University, where he is currently a Professor with the School of Electronic Information and Electrical Engineering. His current research interests include power quality, load modeling, smart grids, microgrid, and intelligent algorithms. He was a recipient of the IEEE Industrial Application Society Prize Paper Award in 2016.

HONG LIU received the B.S., M.S. and Ph.D. degree in electrical engineering from Tianjin University in 2002, 2005 and 2009, respectively. He is currently a Professor with the School of Electrical and Information Engineering, Tianjin University. His research interests include planning, operation simulation and analysis in smart distribution system and integrated energy system. He has contributed to a number of research projects granted from National Natural Science Foundation of China and industry corporations as principal investigator. He has published more than 40 peer-reviewed academic papers and holds more than 10 invention patents of China. Prof. Liu has been a reviewer of IEEE Transactions on Power System, IEEE Transactions on energy conversion and Applied Energy.

Zhidong Cao is an Associate Professor at the State Key Laboratory of Management and Control for Complex Systems, Institute of Automation, Chinese Academy of Sciences. His research interests include public health big data and infectious disease informatics.

Yuankai Bian received the B.Eng. degree in electrical and electronic engineering from Huazhong University of Science and Technology, Wuhan, China, and the University of Birmingham, U.K., in 2013; and the MSc and PhD degrees in Electrical Engineering from the University of Bath, U.K., in 2014 and 2019. He is currently a postdoc research associate with the University of Bath. His research interests include the optimisation of power system operation and planning, and power system economics.

Shuangqi Li was born in Beijing province, China. He received the B.Eng. degree in vehicle engineering from Beijing Institute of Technology, Beijing, China, in 2018. He worked as a research assistant at the National Engineering Laboratory for Electric Vehicles, Beijing Institute of Technology from 2018 to 2019. Currently, he is pursuing the Ph.D. degree at the Department of Electronic and Electrical Engineering, University of Bath. His major research interest is the big data analysis, deep-learning algorithm, operation and planning of smart grid system and V2G service.